15TH IEA HEAT PUMP CONFERENCE
MAY 26–29, 2026 | HOFBURG
VIENNA 2026
DECARBONISATION THROUGH INNOVATION

Design and optimization of a cascaded rooftop heat pump with a centrifugal compressor for cold climates

Yuanzhi Yang[a], Abd Alrhman Bani Issa[a], Bo Shen[b], Davide Ziviani[a]

[a]Ray W. Herrick Laboratories, School of Mechanical Engineering, Purdue University, West Lafayette, IN 47907, USA
[b]Oak Ridge National Laboratory, Oak Ridge, TN 37830, USA

Abstract

With the competitive landscape of the HVAC market characterized by high-performance systems and diverse global regulations for refrigerants, achieving competitiveness requires integrating advanced systems. Conventional rooftop heat pumps (RTHPs) often face significant challenges in severe cold climates, including capacity reduction and increased compressor discharge temperatures. To address these limitations, this study explores an advanced cascaded cold-climate rooftop heat pump (CCRTHP) architecture that utilizes ultra-low GWP refrigerants. Specifically, it employs R1234ze(E) in the upper stage with a small-sized centrifugal compressor, and CO_2 in the lower stage with scroll compressors. Given the inherent lower pressures and reduced volumetric capacity of R1234ze(E), meeting thermal capacity targets demands increased volumetric flow rates and larger system footprints. Additionally, while CO_2 refrigerant excels in heating performance, its efficiency diminishes during cooling operations due to supercritical operations at elevated ambient temperatures. Overcoming these challenges necessitates detailed design and optimization studies.
System-level optimizations were conducted to identify the optimal configurations for heat exchangers, compressor displacement volumes, rotational speeds, and necessary efficiencies across various design conditions. A high-fidelity steady-state cycle model was employed to conduct parametric analyses and component sizing, while a dynamic cycle model was used to investigate control strategies. Preliminary findings indicate a rated cooling coefficient of performance (COP) of 3.1 at a nominal capacity of 70.3 kW (20 tons), alongside a heating COP of 4.0 at the rated conditions. Additionally, the system retains 100% of rated capacity with a COP of 2.4 at -15 °C ambient temperature. These results highlight the potential of cascaded CCRTHP systems as efficient, economically viable solutions for demanding cold climates.

Keywords: Cascade Heat Pump; Rooftop Heat Pump Unit; Cold Climae; Centrifugal Compressor; CO_2

1. Introduction

Commercial buildings in cold-climate regions experience high heating energy demand, frequently relying on electrical resistance heating or gas furnaces because packaged rooftop units (RTUs) cannot reliably meet the loads in extreme conditions. Field evaluations and simulation studies of cold-climate air-source heat pumps indicate extensive use of supplemental electric resistance heating during winter months in colder climates [1].

Single-stage vapor-compression heat pumps suffer performance degradation at low ambient conditions. Research findings showed that heating capacity decreases substantially as outdoor air temperature falls below 4 °C, with particularly severe degradation occurring between -10 °C and -15 °C [2]. The fundamental mechanism involves declining suction pressure coupled with increased temperature lift requirements. This results in elevated compressor work, reduced volumetric efficiency, and diminished capacity due to lower refrigerant density at the suction inlet. Shen et al. [3] reported that heating capacity in conventional units can drop to approximately 20–40% of the rated value at temperatures as low as -25 °C. Consequently, conventional systems either grossly underperform or default to backup heating modes in cold climates.

Architecture optimization is required to address these limitations. The technical literature identifies several promising approaches, including two-stage and cascade compression, vapor injection enhancement, variable-speed compressor implementation, and enlarged outdoor coils with improved heat exchanger designs. Studies particularly highlight cascade cycles and multi-stage compression as effective solutions for low ambient conditions, specifically for evaporator temperatures ranging from -35 °C to -5 °C [4]. At the same time, the HVAC industry is undergoing a transition toward low-GWP refrigerants for commercial RTUs.

This study targets ultra-low GWP refrigerants while maintaining high performance standards. Traditional ultra-low GWP refrigerants present implementation challenges due to system limitations, including reduced capacity and elevated operating pressures. The cascade cycle architecture, through fluid separation into two independent loops, enables effective utilization of these refrigerants while mitigating limitations [5].

2. Methodology

2.1. Cycle Architecture

The overall cycle architecture is illustrated in Figure 1. The system is constructed as a two-stage cascade system in which two independent vapor-compression loops are thermally coupled through an intermediate heat exchanger. In the upper loop, the high-temperature stage uses R1234ze(E) and rejects heat to the indoor airstream while absorbing heat from the intermediate heat exchanger. In the lower loop, the low-temperature stage employs CO_2 and rejects heat to the same intermediate heat exchanger while extracting heat from the outdoor air under ultra-low ambient temperatures. In this configuration, the intermediate heat exchanger simultaneously functions as the condenser for the CO_2 stage and the evaporator for the R1234ze(E) stage, thereby defining the intermediate pressure. The cycle can operate as a single-stage system or as a cascade system, depending on outdoor temperature conditions.

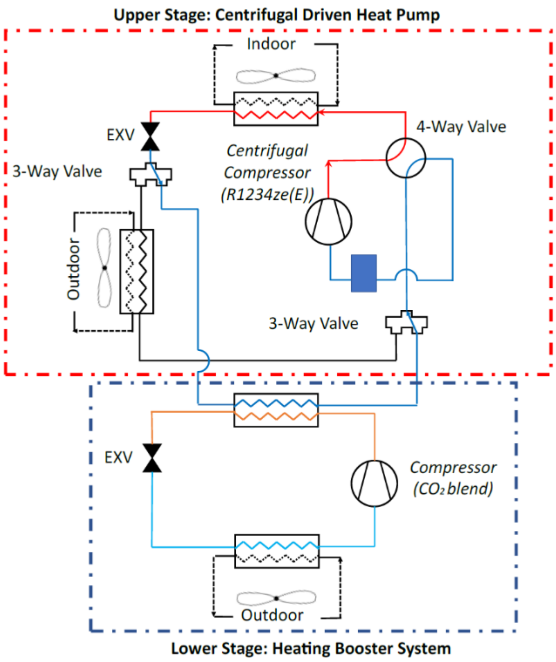

Figure 1. Overall Cycle Architecture

2.2. Modeling Platforms

Steady-state and quasi-steady-state performance were evaluated using the DOE/ORNL Heat Pump Design Model (HPDM), a public-domain research tool that solves mass, energy, and momentum balances for each operating point using detailed thermodynamic and heat-transfer correlations [7]. HPDM was used for component sizing, coil geometry calibration, and generating performance data for bin and building simulations.

To capture the dynamic behavior of the system, including transient responses and mode switching, Dymola/Modelica and the TIL Suite library were used [8]. The dynamic model included finite-volume heat exchanger models, refrigerant charge, compressor maps for both scroll and centrifugal compressors, as well as a control logic. Refrigerant lines were modeled as adiabatic with negligible pressure drop, and oil effects were neglected. Model parameters and design inputs were taken directly from the calibrated HPDM model to ensure consistency between steady-state and dynamic simulations.

2.3. Boundary Conditions and Model Assumptions

Global thermodynamic assumptions were applied consistently across all simulations. Condensers were controlled to maintain a subcooling of 5.6 K (10 °R), while evaporators were controlled for 4.4 K (8 °R) of superheat at the compressor suction. For calibration runs, indoor conditions were held fixed at Air-Conditioning, Heating, and Refrigeration Institute (AHRI) rating conditions, with supply air temperature controlled by the indoor blower and fixed external static pressure. Outdoor relative humidity was considered in frosting corrections for seasonal performance calculations.

The rooftop unit is nominally rated at 70.3 kW (20 tons) of cooling capacity at A1 condition. AHRI Standard 210/240 rating conditions were used as calibration points for both cooling and heating [9]. Rated cooling simulations are performed at 35 °C (95 °F) outdoor dry bulb and 26.7/19.4 °C (80/67 °F) indoor dry/wet bulb conditions with indoor airflow near 3.78 m³/s (8000 CFM) and 249 Pa (1.0 in. w.c.) external static pressure. Heating calibration utilized 8.3 °C (47 °F) outdoor conditions and the same indoor airflow assumption. These boundary conditions also served as the basis for subsequent seasonal and building-level simulations.

Table 1. Baseline 70.3 kW (20 tons) rooftop unit coil geometry

Case	Outdoor DB (°C)	Indoor DB/WB (°C)	Airflow (m³/s)	External static (Pa)	Subcooling (K)	Superheat (K)
Cooling rating (baseline)	35.0	26.7 / 19.4	3.78	249	5.6	4.4
Heating rating (baseline)	8.3	21.1 / –	3.78	249	5.6	4.4
Optimized cascade heating	8.3; -15.0	21.1 / –	per control	per design	3.3	5.6 – 8.3

2.4. Component Modeling

2.4.1. Lower stage CO_2 scroll compressor

The lower-stage compressor is a commercial Copeland CO_2 scroll designed for ultra-low-temperature applications. Its performance was provided as a ten-coefficient fixed-speed map in terms of mass flow rate and power as functions of suction and discharge saturation temperatures. For modeling purposes, the map was used to extract the corresponding volumetric efficiency (η_{vol}) and isentropic efficiency (η_{is}) at given suction ($T_{\text{suc,sat}}$) and discharge ($T_{\text{dis,sat}}$) saturation temperatures.

Variable-speed behavior was implemented by assuming that volumetric efficiency and isentropic efficiency at a given pair of saturation temperatures are independent of rotational speed. The refrigerant mass flow rate ($\dot{m}_{\text{ref}}$) was scaled in proportion to the commanded compressor speed (N) relative to the nominal map speed:

$$\dot{m}_{\text{ref}} = \dot{m}_{\text{map}}\left(T_{\text{suc,sat}}, T_{\text{dis,sat}}\right) \cdot \frac{N}{N_{\text{norm}}} \tag{1}$$

Compressor power (P_{comp}) is then recalculated from the scaled mass flow rate using the same isentropic enthalpy rise and efficiency obtained from the fixed-speed map:

$$P_{\text{comp}} = \frac{m_{\text{ref}} \Delta h_{\text{is}}}{\eta_{\text{is}}} \tag{2}$$

Inverter losses associated with the variable frequency drive were accounted for through power correction. For speeds below 3,600 RPM, the predicted compressor power was multiplied by 1.05, representing a 5% inverter penalty. At 3,600 RPM, the compressor operates without an inverter, so no penalty was applied.

The system employs three identical CO_2 compressors in parallel in the lower stage, all modulated at the same speed. The aggregate electrical power is obtained by multiplying the single-compressor power by 3.15, which accounts for the three parallel units and the 5% inverter loss at part-load speeds.

2.4.2. Upper-stage centrifugal compressor

The upper-stage compressor is modeled as an oil-free centrifugal machine operating with R1234ze(E). The model is theoretical and uses an isentropic efficiency curve from literature. The source is a two-stage heat pump study using an oil-free centrifugal compressor optimized for R134a, where one-dimensional compressor maps are reported as isentropic efficiency versus pressure ratio [6].

In both the HPDM steady-state model and the Dymola dynamic model, the centrifugal compressor is represented using isentropic efficiency as a function of pressure ratio derived from the calibrated map. The cycle solver adjusts the refrigerant mass flow rate implicitly to satisfy the heat balance at the evaporator and condenser for the specified operating point and required capacity.

2.4.3. Heat exchangers and intermediate plate heat exchanger

Heat exchangers were modeled using a combination of detailed coil geometry and empirical correlations embedded in HPDM. The baseline equipment corresponds to a 70.3 kW (20-ton) rooftop unit with one indoor fin-and-tube coil and two outdoor coils. One outdoor coil is dedicated to the upper-stage R1234ze(E) cooling mode, while the second outdoor coil is dedicated to lower-stage CO_2 operation at low ambient temperatures.

Coil circuitry was optimized using HPDM to maximize efficiency at rated conditions. For the upper stage, the outdoor coil configuration was selected to maximize cooling coefficient of performance (COP) of 3.1 at 35 °C (95 °F) ambient and 26.7/19.4 °C (80/67 °F) indoor conditions. Sensitivity analysis showed that upper stage performance is particularly sensitive to suction-side pressure drop, which informed circuit selection and header arrangement. For the lower stage, the CO_2 outdoor coil dedicated to -15 °C (5 °F) ambient heating was optimized for maximum heat transfer at 100% compressor speed. The selected configuration uses three rows and cross-counterflow, which yields a suction saturation temperature near -24.4 °C (-11.9 °F) and enhances overall heating COP. The intermediate plate heat exchanger was modeled implicitly by sizing it to result in a temperature difference of 8.3 K (15 °F) between the condensing CO_2 and evaporating R1234ze(E).

2.5. Preliminary Control and Operating Modes

As shown in Figure 2, the preliminary rule-based control logic is structured around two primary operating configurations: single-stage operation at moderate ambient temperatures and cascade operation at low ambient temperatures.

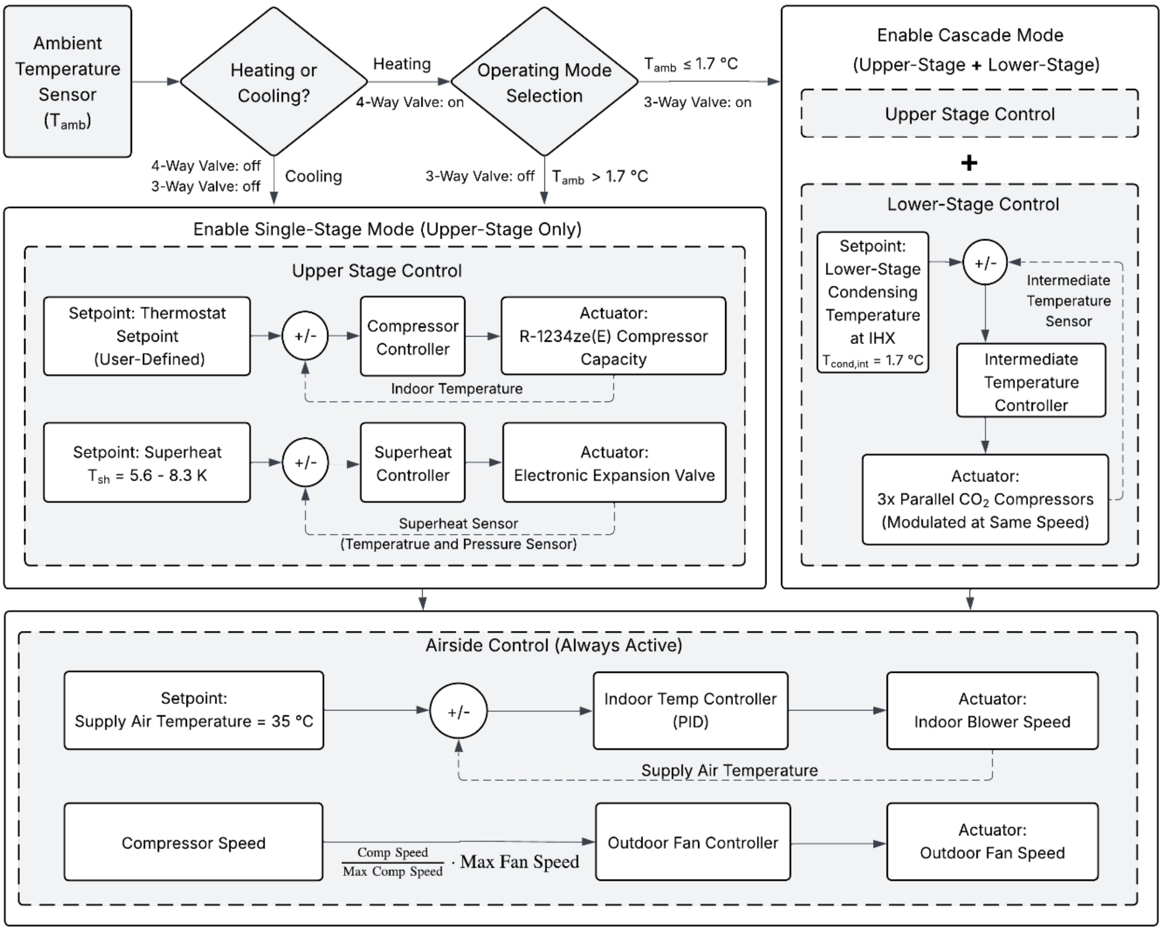

Figure 2. Control and Operation Mode Diagram

In both modes, indoor air temperature is controlled through modulation of the supply fan, and refrigerant-side control targets are maintained through the expansion valves and compressor speeds.

For the upper stage, the R1234ze(E) compressor operates to meet the indoor sensible load while maintaining a suction saturation temperature of -6.7 °C (20 °F). This control target is enforced indirectly through the intermediate plate heat exchanger and the lower-stage condensing temperature. The compressor suction superheat is maintained at approximately 5.6 to 8.3 K (10 to 15 °R) by the electronic expansion valve, and the indoor condenser is controlled to maintain a subcooling degree of 3.3 K (6 °R). Indoor supply air temperature is regulated at 35 °C (95 °F) by varying the indoor blower speed. The blower model assumes constant efficiency ($\eta_{\text{fan}} = 47\%$) and a quadratic relationship between total static head (ΔP) and volumetric airflow rate (Q), resulting in fan power (P_{fan}) scaling with the cube of the airflow rate:

$$P_{\text{fan}} \propto Q^3 \tag{3}$$

Lower-stage controls are primarily based on ambient temperature and intermediate condensation requirements. For outdoor temperatures above 1.7 °C (35 °F), the system operates as a single-stage heat pump. Below this temperature, the system switches to cascade mode, where three parallel CO_2 compressors are modulated to maintain an intermediate condensing temperature of approximately 1.7 °C (35 °F) and a 5.6 K (10 °R) subcooling degree at the plate heat exchanger. The outdoor fan airflow rate is modeled as a linear function of CO_2 compressor speed, reaching 7.55 m^3/s (16,000 CFM) at 3,600 RPM. During cascade operation, the indoor fan continues to modulate to maintain the 35 °C (95 °F) supply air target.

2.6. Verification

Calibration was performed against a baseline 70.3 kW (20-ton) rooftop heat pump to ensure that the modeled system replicates realistic commercial rooftop performance. Manufacturer data provides nominal net capacity, sensible heat ratio (SHR), cooling COP, and coil geometry at the AHRI Standard 210/240 cooling and heating rating points. The HPDM model was configured with the corresponding coil dimensions, airflow rates, and external static pressures.

Calibration adjustments included compressor shell heat loss fractions, which were set to 10% of input power in cooling and 30% in heating, with no cabinet losses. The original compressor map was scaled to match the 70.3 kW (20 tons) capacity while preserving the isentropic efficiency surface. After tuning, simulation results agree closely with the specification table in both modes.

2.7. Frost/Defrost

Seasonal frosting and defrosting effects are incorporated according to AHRI Standard 210/240 guidance for heat pumps. At an ambient condition of 1.7 °C (35 °F) dry bulb and 0.6 °C (33 °F) wet bulb, capacity and power were adjusted using ratios of 0.91 and 0.985, respectively, relative to the steady-state simulation with a clean outdoor coil.

Frost formation was assumed to occur between -8.3 °C (17 °F) and 6.7 °C (44 °F) ambient temperature. For both capacity and power, linear interpolation was applied to obtain degradation factors at intermediate ambient temperatures. Outside this temperature band, frost was assumed negligible.

Additional constraints were incorporated to reflect coil behavior at light frost conditions. Frost formation was suppressed if the compressor speed fell below 1,800 RPM or if the ambient relative humidity was less than 40 %.

2.8. Annual and Bin Analysis

Annual performance was evaluated using AHRI Standard 210/240 climate bins and building load lines. The AHRI framework divides the United States into six climate zones, each characterized by a distinct distribution of heating load hours. Three building load lines were considered: DHR_{min} (well-insulated), DHR_{max} (poorly insulated), and HSPF2 (typical construction). The HPDM-derived capacity and power maps, including frosting corrections, were integrated over the AHRI bins to determine seasonal electric energy consumption.

2.9. Building-Level Simulation Coupling

To further analyze system performance in a realistic commercial application, the cascade rooftop heat pump is coupled with a building energy model in EnergyPlus. EnergyPlus is a whole-building energy simulation program developed by the U.S. Department of Energy that calculates heating and cooling loads, system response, and energy consumption based on building physics, weather data, and HVAC system characteristics [10]. The building selected was a commercial warehouse prototype located in Rochester, Minnesota, a site chosen for its relevance to cold-climate conditions. The warehouse was controlled to maintain a 21.1 °C (70 °F) indoor air temperature in all zones, and the rooftop unit is sized to meet the design heating load at an ambient temperature of -25 °C (−13 °F).

During operation, the building heating load from EnergyPlus was met by modulating the compressor speeds between 600 and 3,600 RPM. At an ambient temperature of approximately 1.7 °C (35 °F), the system transitions from single-stage R1234ze(E) operation to cascade operation. If the CO_2 compressors reach their maximum speed and the building load still exceeds the available capacity, an auxiliary heater is activated.

2.10. Economic and Carbon Calculation Method

Utility cost and carbon emissions were computed using the seasonal energy consumption from bin and building simulations. Natural gas consumption for the reference furnace is calculated assuming that 2.83 m^3 (100 ft^3) of gas yields 105.5 MJ (100,000 Btu) of heating energy and that 28.3 m^3 (1,000 ft^3) of gas costs 10 USD. The baseline furnace was modeled with Annual Fuel Utilization Efficiency (AFUE) values between 70 and 90%. Electricity was priced at 0.10 USD per kWh.

Carbon emissions for natural gas were computed using a fixed emission factor of 181.1 g CO_2 per kWh of delivered heating energy. For electricity, state-level carbon intensities were used to account for regional variations in generation mix.

2.11. Dymola Modelling

Dynamic modeling of the cascaded rooftop heat pump in Dymola was carried out using the same design parameters and component inputs as the HPDM steady-state model. Single-stage and cascaded operation modes were first implemented as separate subsystems to facilitate early testing. Steady boundary-condition simulations were performed in the dynamic environment and compared directly with the HPDM results for representative single-stage and cascade operating points. Under these conditions, the dynamic model reproduced the HPDM predictions for heating capacity, power input, and key saturation temperatures with good agreement, confirming that the underlying thermodynamic behavior was preserved.

3. Results

3.1. Component-Level Performance

Component-level performance analysis of the lower-stage CO_2 compressor indicates that isentropic efficiency exceeds 0.55 at the design evaporating temperature near -15 °C and condensing temperature near 1.7 °C. As the condensing temperature increases toward 21.1 °C to 23.9 °C, the efficiency decreases due to the elevated pressure ratio, peaking around 0.58. The derived efficiency maps, incorporating a 5% power penalty for variable-frequency-drive losses at part-load conditions, are presented in Figure 3.

For the upper stage, the centrifugal compressor performance was calibrated against experimental results. While literature data suggested potential efficiencies up to 77%, the calibration to specific hardware yielded a conservative maximum overall energy efficiency of 72%.

The scaled centrifugal compressor efficiency (η) as a function of pressure ratio (x) is described by the equation:

$$\eta = 0.0.1061x^4 - 0.1908x^3 + 1.136x^2 - 2.669x + 2.773 \quad (4)$$

The resulting performance curve indicates that peak efficiency occurs between pressure ratios of 3.5 and 4.5, which corresponds to the operating conditions of the two-stage design.

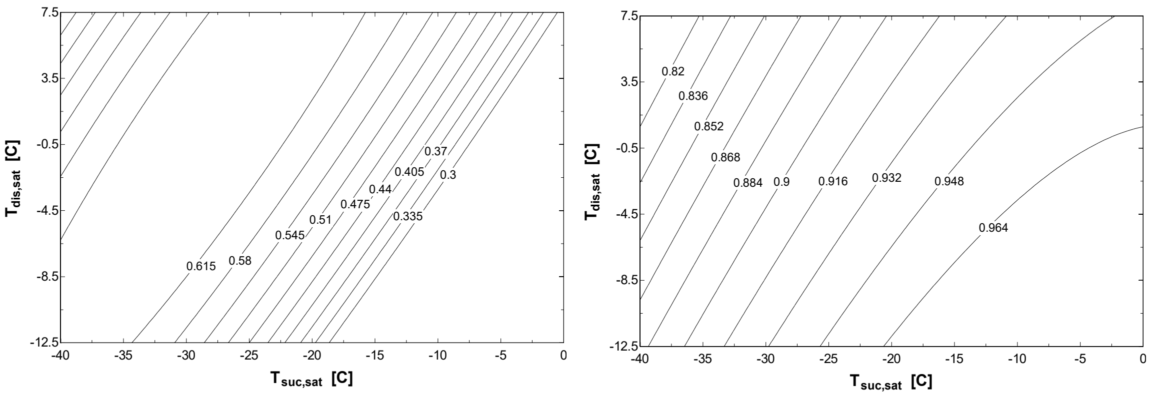

(a) Isentropic Efficiency (b) Volumetric Efficiency

Figure 3. Efficiency of lower-stage CO_2 compressor

3.2. Baseline 70.3 kW Rooftop Unit Calibration

Calibration of the baseline 70.3 kW rooftop unit confirmed the coil geometries and fan characteristics required to match manufacturer performance data.

The model achieved strong agreement with manufacturer specifications under AHRI rating conditions. In cooling mode (35 °C / 95 °F outdoor), the simulated net capacity and cooling COP matched the target values of 70.3 kW (240,000 Btu/h) and 10.9, respectively, within a 1 % margin. Similarly, heating mode calibration at 8.3 °C (47 °F) outdoor temperature reproduced the rated capacity and a COP of 3.43, closely aligning with the specified 3.50. Table 2 presents the detailed comparison between the manufacturer data and the calibrated simulation results.

3.3. Optimized Cascade Configuration and Design Point

Optimization of the coil circuitry for the upper-stage R1234ze(E) system identified a configuration that maximizes cooling COP at rated conditions. The analysis determined that an outdoor coil comprising three rows with 29 parallel circuits in cross-counterflow, combined with an indoor coil of four rows and 58 parallel circuits in cross mixed-flow, yields optimal performance. These circuitry configurations were applied within the established footprint of the baseline 70.3 unit.

For the lower-stage CO_2 outdoor coil, optimization at -15 °C ambient temperature resulted in a three-row, 29-parallel-circuit configuration. This design maximized heat transfer, yielding a suction saturation temperature of approximately -24.4 °C. Furthermore, the optimization of the intermediate cycle conditions revealed that maintaining an upper-stage suction saturation temperature of -6.7 °C results in the highest total heating COP while allowing the system to achieve 100% heating capacity at the -15 °C design condition.

Table 2. Comparison between manufacturer data and calibrated model performance

Parameter	**Specification**	**Simulation**
Cooling Mode		
Net Capacity (kW)	70.3	70.8
SHR (%)	78.6	79.1
Cooling COP	3.19	3.17
Evaporating Temperature (°C)	N/A	11.8
Condensing Temperature (°C)	N/A	51.1
Heating Mode		
Net Capacity (kW)	63.9	63.7
COP	3.50	3.43
Evaporating Temperature (°C)	N/A	-0.4
Condensing Temperature (°C)	N/A	43.1

3.4. Heating and Cooling Performance Versus Ambient Temperature

The predicted heating performance of the optimized 70.3 kW system is illustrated in Figure 4. At an ambient temperature of 8.3 °C (47 °F), the system achieves a heating COP of 4.0. At -15 °C (5 °F), the COP decreases to 2.4. The analysis confirms that to maintain 100% of the required heating capacity at -15 °C (5 °F), the rated thermal heat pump size would need to exceed 70.3 kW.

In cooling mode, operating at 35 °C outdoor dry bulb and 26.7/19.4 °C indoor conditions, the cascade rooftop heat pump achieves a cooling COP of 3.14 at a nominal 70.3 kW capacity. This confirms the system meets targeted cooling performance requirements.

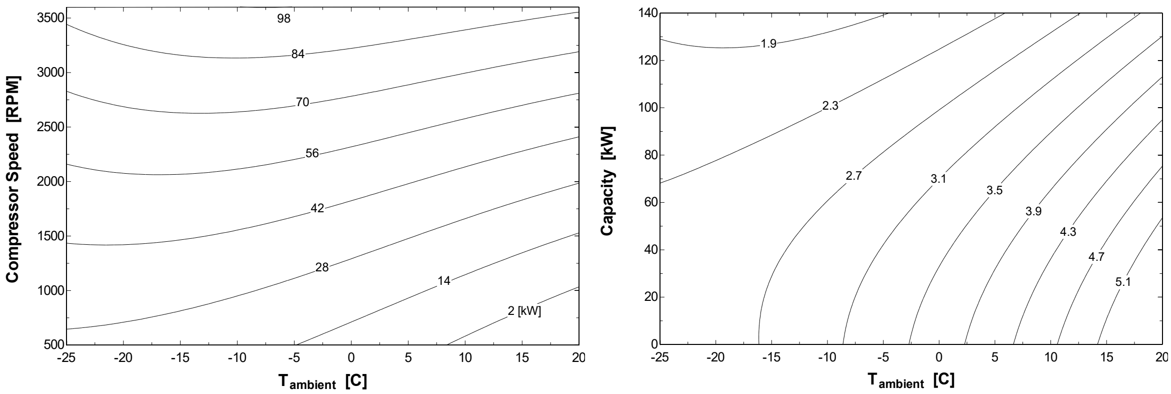

(a) Heating capacity (b) Heating COP

Figure 4. Predicted heating capacity and COP

3.5. Seasonal Bin Analysis and National Performance

Seasonal performance simulations incorporating AHRI Standard 210/240 frosting corrections demonstrate significant utility cost reductions compared to a baseline natural gas furnace with 80% AFUE. As shown in Figure 5, cost savings range from 15% for poorly insulated buildings in cold climates (Region 5) to 50% for well-insulated buildings in milder climates (Region 1). Cost reductions remain evident across all US states, particularly for better-insulated structures. Comparisons against a 90% AFUE furnace indicate reduced but still substantial savings, particularly in warmer zones.

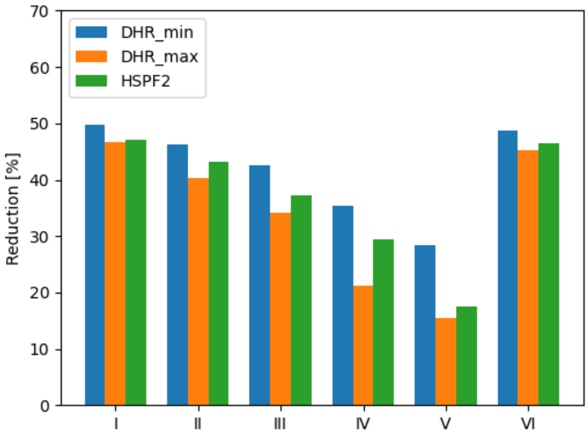

Figure 5. Heating utility cost reductions versus 80% AFUE furnace by AHRI climate zone

State-level analysis of carbon emissions reveals that the cascaded heat pump substantially reduces CO_2 output in most regions compared to an 80% AFUE furnace. However, in states relying on carbon-intensive electricity generation, specifically North Dakota, Wyoming, Utah, Indiana, West Virginia, and Kentucky, the results indicate a net increase in CO_2 emissions. These state-level variations are presented in Figure 6.

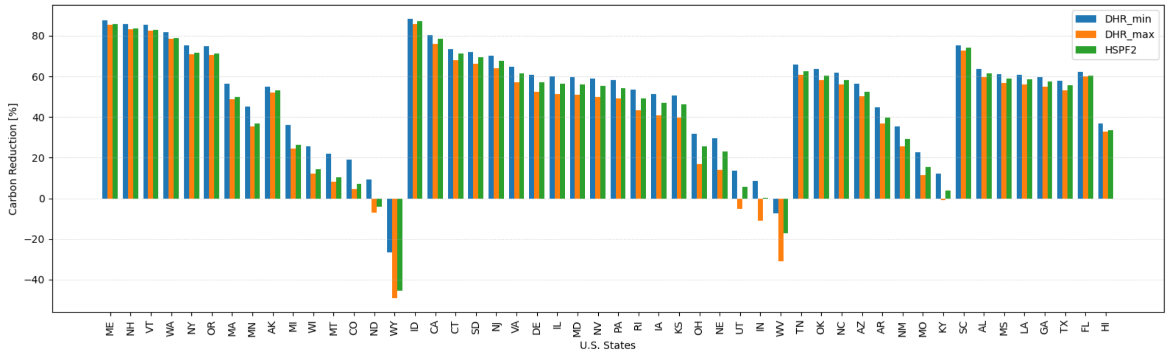

Figure 6. State-level CO_2 emission changes for cascaded heat pump versus 80 % AFUE furnace

3.6. Building-Level Performance in a Cold-Climate Warehouse

Simulations of a commercial warehouse in Rochester, Minnesota, demonstrate the system's dynamic response to cold-climate heating loads. Figure 7 illustrates the required compressor speeds to maintain a 21.1 °C indoor temperature. The results show a clear transition from single stage to cascaded operation at an ambient temperature of approximately 1.7 °C.

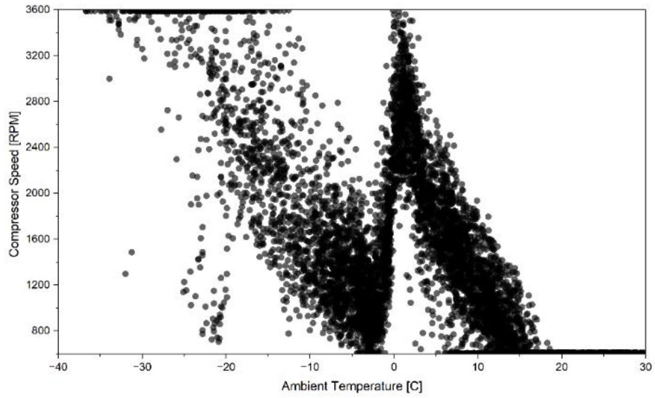

Figure 7. Required compressor speed versus ambient temperature in a warehouse application

Figure 8 presents the integrated heating COP, accounting for auxiliary heat usage. For ambient temperatures below approximately −28.9 °C, conditions that occur less than 1% of the time in the selected location, the integrated COP is limited to about 1.3 due to auxiliary heat usage. Over the remainder of the heating season, the cascaded heat pump maintains significantly higher COP values, particularly in the temperature range where cascade operation is active.

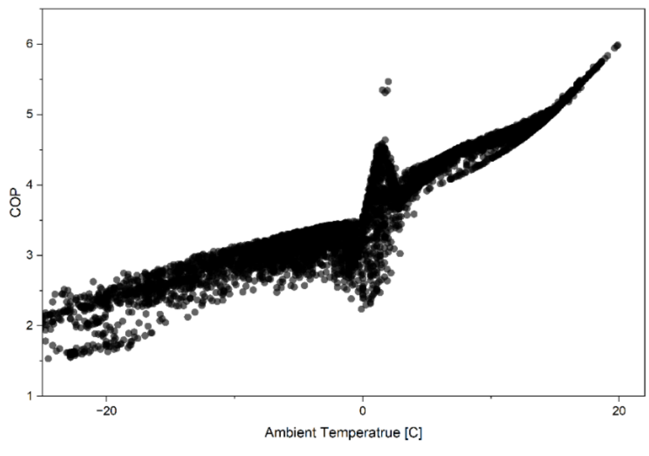

Figure 8. COP versus ambient temperature in warehouse application

Seasonal cost savings for the warehouse application were evaluated by comparing the high-efficiency cascaded heat pump to furnaces with AFUE ratings from 70% to 90%. The analysis indicates that cost reductions exceed 15% even when compared to high-efficiency furnaces in a cold climate, with larger savings in milder climate zones or for buildings closer to the DHR_{min} load line. These building-level results are consistent with the national climate-zone analysis and support the economic viability of the cascade configuration.

3.7. Dynamic Model Validation

The dynamic system model was successfully implemented to evaluate transient behavior and control loop stability. Active Proportional-Integral (PI) control strategies were enabled within the simulation to regulate component operation. The complete dynamic cycle architecture utilized for these simulations is illustrated in Figure 9.

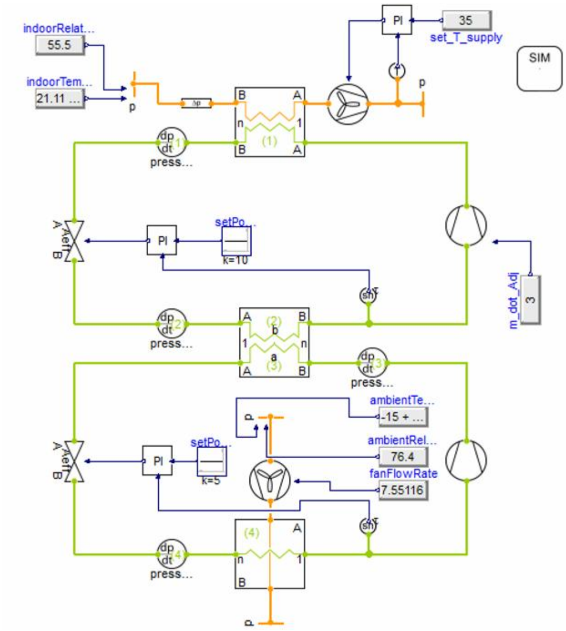

Figure 9. Dymola Model

Control to validate dynamic formulation, simulations were conducted to observe the system's temporal response. Figure 10 presents the evolution of heating capacity and COP over time. The results demonstrate that the control logic effectively stabilizes the system; notably, once the transient effects subside and the system reaches a steady operating state, the resulting performance metrics align with the steady-state predictions derived from the HPDM model.

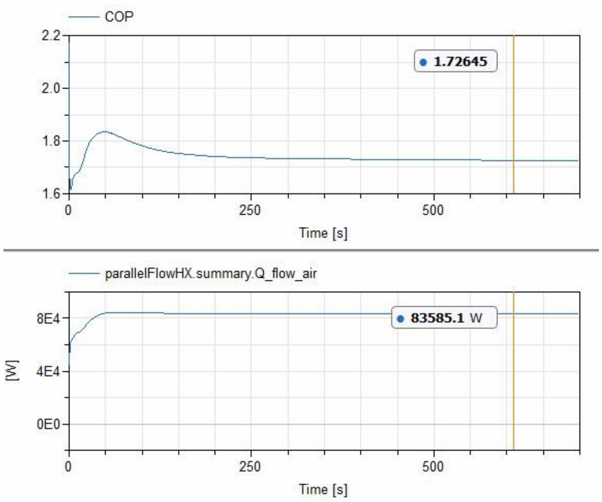

Figure 10. Performance for steady-state operations.

4. Discussion

The simulation results indicate that the cascade architecture successfully mitigates the thermodynamic limitations typically observed in single-stage air-source heat pumps. By decoupling the total temperature lift, the system avoids the severe reduction in volumetric efficiency and capacity often seen at ambient temperatures below -10 °C. The ability to maintain a COP of 2.4 at -15 °C implies that the selected intermediate saturation temperature of -6.7 °C appropriately balances the compression ratio between the lower-stage CO_2 scroll compressors and the upper-stage R1234ze(E) centrifugal compressor.

Economic analysis suggests that the proposed system represents a viable pathway for the electrification of commercial heating. Utility cost reductions exceeding 15%, even in the coldest climate zones, indicate that the efficiency gains of the cascade system outweigh the higher unit cost of electricity relative to natural gas. However, the environmental assessment reveals that decarbonization is not intrinsic to the equipment alone but is contingent upon the carbon intensity of the local electrical grid. The increase in CO_2 emissions observed in states with carbon-intensive generation highlights that the widespread deployment of such high-efficiency heat pumps must be coordinated with grid modernization efforts to achieve net emission reductions.

To ensure the highest fidelity in performance prediction, both the high-stage centrifugal compressor and the low-stage CO_2 compressors will undergo comprehensive experimental validation. This hardware testing will generate actual performance maps derived directly from the specific operating conditions of the cascade cycle. These experimentally validated maps will replace the initial modeling inputs, thereby ensuring that the simulation results represent real-life outcomes and accurately reflect the efficiency characteristics of the final system configuration.

Future work will focus on integrating load-based testing within the Dymola framework to evaluate system response under fluctuating building demands rather than fixed ambient bins. A physical field test of the complete system will be conducted to validate the transient response of refrigerant lines and heat exchangers, which were modeled as ideal components in this study.

Acknowledgements

This material is based upon work supported by the U.S. Department of Energy's Office of Energy Efficiency and Renewable Energy (EERE) under the BENEFIT 2023 award number DE-EE0010925. This report was prepared as an account of work sponsored by an agency of the United States Government. Neither the United States Government nor any agency thereof, nor any of their employees, makes any warranty, express or implied, or assumes any legal liability or responsibility for the accuracy, completeness, or usefulness of any information, apparatus, product, or process disclosed, or represents that its use would not infringe privately owned rights. Reference herein to any specific commercial product, process, or service by trade name, trademark, manufacturer, or otherwise does not necessarily constitute or imply its endorsement, recommendation, or favoring by the United States Government or any agency thereof. The views and opinions of authors expressed herein do not necessarily state or reflect those of the United States Government or any agency thereof.

References

[1] Gschwend, A., Menzi, T., Caskey, S., Groll, E.A., Bertsch, S.S., 2016. Energy consumption of cold climate heat pumps in different climates – Comparison of single-stage and two-stage systems. International Journal of Refrigeration 62, 193–206. https://doi.org/10.1016/j.ijrefrig.2015.10.003

[2] Bertsch, S.S., Groll, E.A., 2008. Two-stage air-source heat pump for residential heating and cooling applications in northern U.S. climates. International Journal of Refrigeration 31, 1282–1292. https://doi.org/10.1016/j.ijrefrig.2008.01.006

[3] Shen, B., Abdelaziz, O.A., Rice, C.K., Baxter, V.D., Pham, H., 2016. Cold climate heat pumps using tandem compressors. In: Proceedings of the 2016 ASHRAE Winter Conference, Orlando, FL, USA, January 2016. Paper OR-16-C039.

[4] Yang, X., Wang, B., Cheng, Z., Shi, W., Yu, Y., 2021. Upper-limit of performance improvement by using (quasi) two-stage vapor compression. Applied Thermal Engineering 185, 116426. https://doi.org/10.1016/j.applthermaleng.2020.116426

[5] Llopis, R., Sánchez, D., Sanz-Kock, C., Cabello, R., Torrella, E., 2015. Energy and environmental comparison of two-stage solutions for commercial refrigeration at low temperature: Fluids and systems. Applied Energy 138, 133–142. https://doi.org/10.1016/j.apenergy.2014.10.069

[6] Arpagaus, C., Bertsch, S., Javed, A., Schiffmann, J., 2016. Two-Stage Heat Pump using Oil-Free Turbocompressors - System Design and Simulation.
[7] DOE/ORNL Heat Pump Design Model (HPDM) [WWW Document], n.d. URL https://hpdmflex.ornl.gov/hpdm/wizard/welcome.php
[8] TLK-Thermo GmbH, 2024. TIL Suite, version 2024.1 [Software]. TLK-Thermo GmbH. URL https://www.tlk-thermo.com/en/software/til-suite
[9] AHRI, 2024. AHRI Standard 210/240-2024 (I-P), Performance Rating of Unitary Air-conditioning and Air-source Heat Pump Equipment. Air-Conditioning, Heating, and Refrigeration Institute, Arlington, VA.
[10] EnergyPlus [WWW Document], n.d. . Energy.gov. URL https://www.energy.gov/eere/buildings/articles/energyplus